Available online at www.sciencedirect.com
ScienceDirect
Physica E 40 (2008) 2352–2359
PHYSICA E
www.elsevier.com/locate/physe

Optical properties of nanotube bundles by photoluminescence excitation and absorption spectroscopy

P.H. Tan[a,b,*], T. Hasan[a], F. Bonaccorso[a,c], V. Scardaci[a], A.G. Rozhin[a], W.I. Milne[a], A.C. Ferrari[a]

[a]*Department of Engineering, University of Cambridge, Cambridge CB3 0FA, UK*
[b]*State Key Laboratory for Superlattices and Microstructures, P.O. Box 912, Beijing 100083, China*
[c]*CNR-Istituto per i Processi Chimico-Fisici and Dipartimento di Fisica della Materia e Tecnologie Fisiche Avanzate, Universita' di Messina, 98166 Messina, Italy*

Available online 25 October 2007

Abstract

Photoluminescence excitation (PLE) and absorption spectroscopy are applied to investigate the impact of bundle size on the optical properties of single wall carbon nanotube (SWNT) bundles in aqueous suspensions. The existence and gradual formation of small bundles happens in aqueous suspensions even after ultrasonication and ultracentrifugation. With time, the emission and absorption spectra show weaker intensities and broader spectral profiles, confirming the formation of bigger SWNT bundles. We detect new PLE features assigned to energy transfer from excitons and excitonic phonon sidebands of donors to eh_{11} excitons of acceptors in such suspensions. In addition, the photoluminescence intensity from large gap nanotube donors weakens, while that from the smaller gap acceptors increases because of the exciton energy transfer. Our results caution the use of photoluminescence to determine the abundance of different SWNT species in conventionally prepared aqueous suspensions. On the contrary, absorption measurements represent a more reliable technique to reveal such information.

PACS: 78.55.Cr; 71.20.Nr; 73.20.Jc; 78.67.De

Keywords: Photoluminescence excitation; Absorption; Bundle; Carbon nanotube

1. Introduction

Single wall carbon nanotubes (SWNTs) are model systems for the investigation of fundamental physics in one dimension. Excitons dominate the optical response of SWNTs even at room temperature [1,2]. Absorption and photoluminescence (PL) have been successfully applied to characterize the optical properties and excitonic transitions of SWNTs in dispersed and micelle-encapsulated SWNT suspensions [3,4]. In recent years, many works focused on isolated SWNT suspensions assuming that ultracentrifugation would completely remove SWNT bundles [5,6]. However, very small bundles with about 3–10 tubes inevitably exist in most of the aqueous micelle-like SWNT suspensions even after conventional ultrasonication followed by ultracentrifugation. We recently investigated photoluminescence excitation (PLE) in nanotube bundles [7]. We found that exciton energy transfer (EET) between adjacent nanotubes enhances PL emission from small gap nanotube acceptors [7].

Here, we investigate and compare the optical properties of as-prepared SWNT suspensions and after 2 months of incubation by absorption and PLE spectroscopy. We discuss the changes in optical characteristics upon formation of bundles. The new features observed in PLE can be explained by EET and are assigned in detail.

*Corresponding author. Department of Engineering, University of Cambridge, Cambridge CB3 0FA, UK. Tel.: +44 1223 748368; fax: +44 1223 748348.
E-mail address: pt290@eng.cam.ac.uk (P.H. Tan).

1386-9477/$ - see front matter © 2007 Elsevier B.V. All rights reserved.
doi:10.1016/j.physe.2007.10.058

2. Experiment

We perform absorption and PLE measurements on CoMoCAT SWNT (South West Nanotechnologies) suspensions in D_2O with sodium dodecylbenzene sulfonate (SDBS) as surfactant. A procedure similar to that reported in Ref. [8] is used to prepare SWNT solutions with 1.0 wt% SDBS. Absorption spectra are measured with a Perkin-Elmer Lambda 950 spectrometer. A HORIBA Jobin Yvon Fluorolog-3 with double-grating excitation monochromator, single-grating emission monochromator, InGaAs near-IR detector and CCD is used for PLE measurements. PLE maps are collected with a 6-nm bandpass slit for both monochromators. Data are corrected for excitation intensity.

3. Results and discussions

Fig. 1 plots PLE maps of the as-prepared suspension (left panel, (a1) and (a2) and of the same suspension after 2 months (right panel, (b1) and (b2)) in the emission range 930–1160 nm and in the excitation ranges 500–680 nm and 930–990 nm. Each resonance spot in Figs. 1(a1), (a2), (b1) and (b2) is labeled with (λ_{ex}, λ_{em}), where λ_{em} and λ_{ex} are the emission and excitation wavelengths, respectively. Several strong intensity peaks in Fig. 1 are exciton–exciton resonances [4,8]. The positions of these resonances originally observed in Ref. [4] are indicated with crosses. We note that the eh_{11} emission of SWNTs in Figs. 1(a1) and (a2) are red-shifted by about 1–5 nm relative to those in Ref. [4], consisting of sodium dodecyl sulfate (SDS) aided SWNT suspensions. Nanotube suspensions [9] prepared with the similar methods using SDS and SDBS do not display any spectral shift. Therefore, the effect of dielectric screening on individual SWNTs by SDS and SDBS are nearly identical within the emission range 850–1100 nm. Hence, compared to previous results [4], we assume the red-shifts in the emission wavelengths in our sample to reflect the presence of nanotube bundles.

Theoretical calculations show that phonon sidebands appear in PLE maps, peaking at about 210 meV above the excitonic line [12]. The (8,3), (6,5), (7,5) and (8,4) tubes exhibit such features above their eh_{22} transitions in Fig. 1(a2). The calculated phonon sidebands of eh_{11} for (8,3), (6,5), (7,5), (7,6) and (8,4) tubes based on Ref. [12] are indicated in Fig. 1(a2) by open diamonds. Some features in Figs. 1(a1), (a2) indicated by arrows, however, cannot be assigned to any exciton–exciton resonance or phonon sideband. Interestingly, their excitation corresponds to the eh_{11} or eh_{22} of one nanotube species, but their emission energy matches another. This implies that resonant excitation of large gap donor semiconducting SWNTs (s-SWNTs) induces emission from smaller gap acceptor s-SWNTs adjacent to each other, most likely in same bundle [7].

In the PLE map from the same suspension sealed for 2 months (Figs. 1(b1) and (b2)), the eh_{11} wavelength of each resonance further red-shifts by about 1–5 nm relative to the as-prepared suspensions shown in Figs. 1(a1) and (a2). This strongly suggests further aggregation of dispersed SWNTs into bigger bundles after 2-months [10,11]. Another sign of SWNT aggregations is that all the exciton–exciton resonances decrease in intensity after 2 months. However, the intensity of the EET feature at (982 nm, 1122 nm) is stronger than that of the as-prepared suspension. Compared to Fig. 1(a2), the corresponding

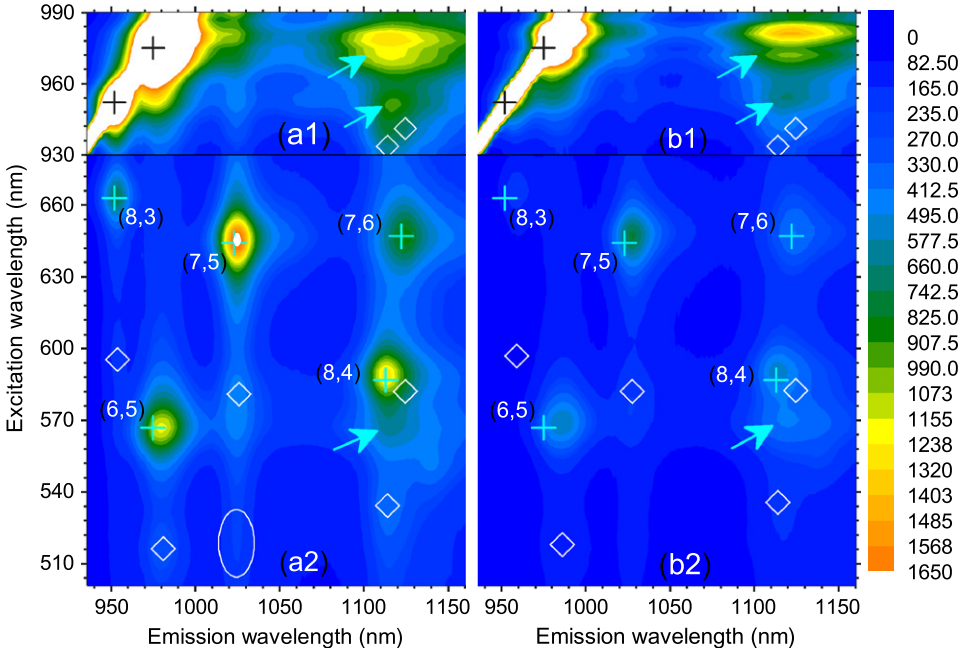

Fig. 1. (Color online). PLE maps for (a1, a2) as-prepared suspensions and (b1, b2) after 2 months. The (n, m) assignments are shown. Crosses indicate the corresponding exciton–exciton resonances observed in Ref. [4]. Arrows and ellipses show the new PLE features assigned to EET [7].

EET peak in Fig. 1(b2) at (571 nm, 1120 nm) can be identified more clearly due to the lower intensity of the (eh_{22}, eh_{11}) of (8,4) tubes in the latter map. The PLE feature associated with the (7,5) emission extends to 516 nm. This corresponds to the energy of eh_{22} phonon sidebands in (6,5) tubes. In suspensions with isolated nanotubes, the exciton–exciton resonances rapidly decrease in intensity when the excitation is non-resonant with the excitonic states [4,8]. This is also true for PLE features where energy transfer between nanotubes in bundles takes place (e.g., the EET peak near (980 nm, 1120 nm) in Figs. 1(a1) and (b1)), and also for PLE features of phonon sidebands [13,14]. In Fig. 1(a2), the PLE feature near (517 nm, 1025 nm) indicated by an ellipse is associated with the resonant excitation of a eh_{22} (6,5) sideband and emission from eh_{11} of (7,5). This suggests that this feature could originate due to energy transfer from the excitonic sidebands of the eh_{22} excitons of (6,5) donors to eh_{11} of (7,5) acceptors.

The complete PLE map from the as-prepared SWNT suspension is shown in Fig. 2. In contrast to the suspensions of isolated nanotubes [4,8], the spectral profile of our exciton resonances significantly elongates in the horizontal and vertical directions. A thorough examination of all the features in Fig. 2 allows us to identify several energy transfer features from excitons (crosses in Fig. 2) or phonon sidebands (× in Fig. 2) of donors to excitons of acceptor nanotubes. The assignments of the exciton–exciton resonances, excitonic phonon sidebands and the corresponding EET are, in detail, summarized in Tables 1 and 2. Although the PL emission from (5,4) donor tubes is very weak in Fig. 2 when their eh_{11}, eh_{22} and corresponding sidebands are resonantly excited, the PL features due to energy transfer from (5,4) donor tubes can be identified, as indicated in Fig. 2 by horizontal dashed lines. This implies that the energy transfer efficiency from donors to acceptors could be very high when the donor exciton states and their phonon sidebands are resonantly excited [7].

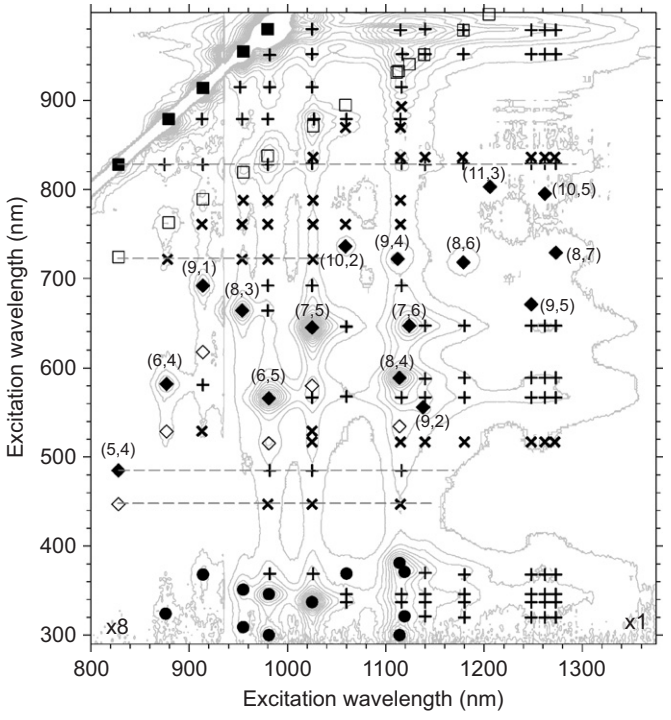

Fig. 2. PLE map of as-prepared SWNT suspension. Solid squares, diamonds and circles represent eh_{11} emission of SWNTs for excitation matching their eh_{11}, eh_{22}, eh_{33} and eh_{44}. Each (eh_{22}, eh_{11}) resonance is labeled with the chiral index of the corresponding SWNT. Open squares and diamonds are phonon sidebands. Solid crosses are assigned to EET. Solid × is assigned to energy transfer between sidebands of donors and excitons of acceptors.

To reveal how the PL, PLE and absorption spectra of nanotube bundles change with time, we show the absorption spectra and the PL intensity of each exciton–exciton resonance of as-prepared suspension and of the same suspension after 2 months of incubation in Fig. 3(a). It was reported that the theoretical PL intensity of an individual (6,5) tube is about 20% stronger than that of an individual (7,5) tube [15]. The absorption intensity of (6,5) tubes in suspension is also much stronger than that of (7,5) tubes as shown in Fig. 3(a). Thus, the PL intensity of (6,5) tubes is expected to be stronger than that of (7,5) tubes in suspensions if all nanotubes are individually suspended. However, Fig. 3(a) shows that in our case the (7,5) tubes exhibit much stronger PL emissions. The red-shift in the absorption and PL spectra confirms that the SWNTs in the as-prepared suspension contain small SWNT bundles. Note that the (6,5) absorption peak is broader than that of (7,5) tubes. This implies that the dielectric environment of (6,5) tubes, induced by the larger size distribution of bundles containing the (6,5) tubes, is more complex than that of the (7,5). Compared to isolated nanotubes [4,8], additional EET relaxation channels exist in bundles [7]. Therefore, for suspensions where the presence of bundles and their size distributions cannot be conclusively determined, the (eh_{22}, eh_{11}) intensity of each nanotube species does not necessarily reflect its abundance contrary to what sometimes suggested [5,6], even if the experimental PL spectra are normalized with respect to concentrations and theoretical cross-sections [15]. Considering that the absorption spectra of suspensions sealed for 2 months show a similar profile to that of the pristine suspensions, we conclude that absorption spectroscopy is a more reliable technique to determine the concentration distribution of nanotubes in suspensions.

In order to compare the different contributions of exciton–exciton resonances, phonon sidebands and exciton energy transfer to the PL spectra of the pristine suspension and of the same suspension after 2 months, we sum all the PL spectra in the PLE map in Fig. 2 with excitations between 420 and 780 nm and between 780 and 999 nm into two separate PL spectra. The corresponding summed spectra between 420 and 780 nm and between 780 and 999 nm are depicted in Figs. 3(b) and (c), respectively. Referring to Fig. 2, we find that the spectra in Fig. 3(b) include contributions from almost all the (eh_{22}, eh_{11}) resonances, sidebands and corresponding energy transfers. Among them the (eh_{22}, eh_{11}) resonances are dominant in

Table 1
Assignment of the observed exciton–exciton resonances and corresponding EET features in the PLE map of as-prepared CoMoCAT SWNT suspensions in D_2O/SDBS

$(\lambda_{ex}, \lambda_{em})$	(E_{ex}, E_{em})	(eh_{ii}, eh_{11}) peaks		EET features		
		(n,m)	Assign.	Donor	Assign.	Acceptor
(980,980)	(1.265,1.265)	(6,5)	(eh_{11}, eh_{11})			
(980,1025)	(1.265,1.210)			(6,5)	$(eh_{11}^{D}, eh_{11}^{A})$	(7,5)
(980, ~1116)	(1.265,1.111)			(6,5)	$(eh_{11}^{D}, eh_{11}^{A})$	(8,4),(9,4),(7,6)
(980,1139)	(1.265,1.088)			(6,5)	$(eh_{11}^{D}, eh_{11}^{A})$	(9,2)
(980,1180)	(1.265,1.051)			(6,5)	$(eh_{11}^{D}, eh_{11}^{A})$	(8,6)
(980, ~1260)	(1.265,0.984)			(6,5)	$(eh_{11}^{D}, eh_{11}^{A})$	(9,5),(10,5),(8,7)
(955,955)	(1.298,1.298)	(8,3)	(eh_{11}, eh_{11})			
(955,980)	(1.298,1.265)			(8,3)	$(eh_{11}^{D}, eh_{11}^{A})$	(6,5)
(955,1025)	(1.298,1.210)			(8,3)	$(eh_{11}^{D}, eh_{11}^{A})$	(7,5)
(955, ~1116)	(1.298,1.111)			(8,3)	$(eh_{11}^{D}, eh_{11}^{A})$	(8,4),(9,4),(7,6)
(955,1139)	(1.298,1.088)			(8,3)	$(eh_{11}^{D}, eh_{11}^{A})$	(9,2)
(955,1180)	(1.298,1.051)			(8,3)	$(eh_{11}^{D}, eh_{11}^{A})$	(8,6)
(955, ~1260)	(1.298,0.984)			(8,3)	$(eh_{11}^{D}, eh_{11}^{A})$	(9,5),(10,5),(8,7)
(914,914)	(1.357,1.357)	(9,1)	(eh_{11}, eh_{11})			
(914,955)	(1.357,1.298)			(9,1)	$(eh_{11}^{D}, eh_{11}^{A})$	(8,3)
(914,980)	(1.357,1.265)			(9,1)	$(eh_{11}^{D}, eh_{11}^{A})$	(6,5)
(914,1025)	(1.357,1.210)			(9,1)	$(eh_{11}^{D}, eh_{11}^{A})$	(7,5)
(914, ~1116)	(1.357,1.111)			(9,1)	$(eh_{11}^{D}, eh_{11}^{A})$	(8,4),(9,4),(7,6)
(879,879)	(1.411,1.411)	(6,4)	(eh_{11}, eh_{11})			
(879,914)	(1.411,1.357)			(6,4)	$(eh_{11}^{D}, eh_{11}^{A})$	(9,1)
(879,955)	(1.411,1.298)			(6,4)	$(eh_{11}^{D}, eh_{11}^{A})$	(8,3)
(879,980)	(1.411,1.265)			(6,4)	$(eh_{11}^{D}, eh_{11}^{A})$	(6,5)
(879,1025)	(1.411,1.210)			(6,4)	$(eh_{11}^{D}, eh_{11}^{A})$	(7,5)
(879,1060)	(1.411,1.170)			(6,4)	$(eh_{11}^{D}, eh_{11}^{A})$	(10,2)
(879, ~1116)	(1.411,1.111)			(6,4)	$(eh_{11}^{D}, eh_{11}^{A})$	(8,4),(9,4),(7,6)
(828,828)	(1.498,1.498)	(5,4)	(eh_{11}, eh_{11})			
(828,879)	(1.498,1.411)			(5,4)	$(eh_{11}^{D}, eh_{11}^{A})$	(6,4)
(828,914)	(1.498,1.357)			(5,4)	$(eh_{11}^{D}, eh_{11}^{A})$	(9,1)
(828,980)	(1.498,1.265)			(5,4)	$(eh_{11}^{D}, eh_{11}^{A})$	(6,5)
(828,1025)	(1.498,1.210)			(5,4)	$(eh_{11}^{D}, eh_{11}^{A})$	(7,5)
(828, ~1116)	(1.498,1.111)			(5,4)	$(eh_{11}^{D}, eh_{11}^{A})$	(8,4),(9,4),(7,6)
(828,1139)	(1.498,1.088)			(5,4)	$(eh_{11}^{D}, eh_{11}^{A})$	(9,2)
(828,1180)	(1.498,1.051)			(5,4)	$(eh_{11}^{D}, eh_{11}^{A})$	(8,6)
(828, ~1260)	(1.498,0.984)			(5,4)	$(eh_{11}^{D}, eh_{11}^{A})$	(9,5),(10,5),(8,7)
(803,1206)	(1.544,1.028)	(11,3)	(eh_{22}, eh_{11})			
(795,1262)	(1.560,0.982)	(10,5)	(eh_{22}, eh_{11})			
(736,1060)	(1.685,1.170)	(10,2)	(eh_{22}, eh_{11})			
(729,1273)	(1.701,0.974)	(8,7)	(eh_{22}, eh_{11})			
(722,1112)	(1.717,1.115)	(9,4)	(eh_{22}, eh_{11})			
(718,1180)	(1.727,1.051)	(8,6)	(eh_{22}, eh_{11})			
(692,914)	(1.792,1.357)	(9,1)	(eh_{22}, eh_{11})			
(692,980)	(1.792,1.265)			(9,1)	$(eh_{22}^{D}, eh_{11}^{A})$	(6,5)
(692,1025)	(1.792,1.209)			(9,1)	$(eh_{22}^{D}, eh_{11}^{A})$	(7,5)
(692, ~1116)	(1.792,1.111)			(9,1)	$(eh_{22}^{D}, eh_{11}^{A})$	(8,4),(9,4),(7,6)
(671,1248)	(1.848,0.993)	(9,5)	(eh_{22}, eh_{11})			
(664,955)	(1.867,1.298)	(8,3)	(eh_{22}, eh_{11})			
(664,980)	(1.867,1.265)			(8,3)	$(eh_{22}^{D}, eh_{11}^{A})$	(6,5)
(647,1124)	(1.917,1.103)	(7,6)	(eh_{22}, eh_{11})			
(645,1025)	(1.922,1.209)	(7,5)	(eh_{22}, eh_{11})			
(645,1060)	(1.922,1.170)			(7,5)	$(eh_{22}^{D}, eh_{11}^{A})$	(10,2)
(646,1139)	(1.919,1.089)			(7,5)(7,6)	$(eh_{22}^{D}, eh_{11}^{A})$	(9,2)
(646,1180)	(1.919,1.051)			(7,5)(7,6)	$(eh_{22}^{D}, eh_{11}^{A})$	(8,6)
(646, ~1260)	(1.919,0.984)			(7,5)(7,6)	$(eh_{22}^{D}, eh_{11}^{A})$	(9,5)(10,5)(8,7)
(589,1114)	(2.105,1.113)	(8,4)	(eh_{22}, eh_{11})			

Table 1 (*continued*)

$(\lambda_{ex}, \lambda_{em})$	(E_{ex}, E_{em})	(eh_{ii}, eh_{11}) peaks		EET features		
		(n,m)	Assign.	Donor	Assign.	Acceptor
(589,1139)	(2.105,1.089)			(8,4)	$(eh_{22}^{D}, eh_{11}^{A})$	(9,2)
(589,1180)	(2.105,1.051)			(8,4)	$(eh_{22}^{D}, eh_{11}^{A})$	(8,6)
(589, ~1260)	(2.105,0.984)			(8,4)	$(eh_{22}^{D}, eh_{11}^{A})$	(9,5)(10,5)(8,7)
(582,879)	(2.131,1.411)	(6,4)	(eh_{22}, eh_{11})			
(582,914)	(2.131,1.357)			(6,4)	$(eh_{22}^{D}, eh_{11}^{A})$	(9,1)
(566,980)	(2.191,1.265)	(6,5)	(eh_{22}, eh_{11})			
(566,1025)	(2.191,1.209)			(6,5)	$(eh_{22}^{D}, eh_{11}^{A})$	(7,5)
(566,1060)	(2.191,1.170)			(6,5)	$(eh_{22}^{D}, eh_{11}^{A})$	(10,2)
(566, ~1116)	(2.191,1.111)			(6,5)	$(eh_{22}^{D}, eh_{11}^{A})$	(8,4)(9,4)(7,6)
(566,1139)	(2.191,1.089)			(6,5)	$(eh_{22}^{D}, eh_{11}^{A})$	(9,2)
(566,1180)	(2.191,1.051)			(6,5)	$(eh_{22}^{D}, eh_{11}^{A})$	(8,6)
(566, ~1260)	(2.191,0.984)			(6,5)	$(eh_{22}^{D}, eh_{11}^{A})$	(9,5)(10,5)(8,7)
(485,828)	(2.557,1.497)	(5,4)	(eh_{22}, eh_{11})			
(485,980)	(2.557,1.265)			(5,4)	$(eh_{22}^{D}, eh_{11}^{A})$	(6,5)
(485,1025)	(2.557,1.210)			(5,4)	$(eh_{22}^{D}, eh_{11}^{A})$	(7,5)
(485, ~1116)	(2.557,1.111)			(5,4)	$(eh_{22}^{D}, eh_{11}^{A})$	(8,4)(9,4)(7,6)
(381,1114)	(3.254,1.113)	(8,4)	(eh_{33}, eh_{11})			
(300,1114)	(4.133,1.113)	(8,4)	(eh_{44}, eh_{11})			
(371,1119)	(3.342,1.108)	(7,6)	(eh_{33}, eh_{11})			
(371,1139)	(3.342,1.089)			(7,6)	$(eh_{33}^{D}, eh_{11}^{A})$	(9,2)
(371,1180)	(3.342,1.051)			(7,6)	$(eh_{33}^{D}, eh_{11}^{A})$	(8,6)
(371, ~1260)	(3.342,0.984)			(7,6)	$(eh_{33}^{D}, eh_{11}^{A})$	(9,5)(10,5)(8,7)
(321,1119)	(3.863,1.108)	(7,6)	(eh_{44}, eh_{11})			
(321,1139)	(3.863,1.089)			(7,6)	$(eh_{44}^{D}, eh_{11}^{A})$	(9,2)
(321,1180)	(3.863,1.051)			(7,6)	$(eh_{44}^{D}, eh_{11}^{A})$	(8,6)
(321, ~1260)	(3.863,0.984)			(7,6)	$(eh_{44}^{D}, eh_{11}^{A})$	(9,5)(10,5)(8,7)
(369,1060)	(3.360,1.170)	(10,2)	(eh_{33}, eh_{11})			
(368,914)	(3.370,1.357)	(9,1)	(eh_{33}, eh_{11})			
(368,980)	(3.370,1.265)			(9,1)	$(eh_{33}^{D}, eh_{11}^{A})$	(6,5)
(368,1025)	(3.370,1.210)			(9,1)	$(eh_{33}^{D}, eh_{11}^{A})$	(7,5)
(351,955)	(3.533,1.298)	(8,3)	(eh_{33}, eh_{11})			
(309,955)	(4.013,1.298)	(8,3)	(eh_{44}, eh_{11})			
(346,980)	(3.584,1.265)	(6,5)	(eh_{33}, eh_{11})			
(300,980)	(4.133,1.265)	(6,5)	(eh_{44}, eh_{11})			
(346,1060)	(3.584,1.170)			(6,5)	$(eh_{33}^{D}, eh_{11}^{A})$	(10,2)
(346, ~1116)	(3.584,1.111)			(6,5)	$(eh_{33}^{D}, eh_{11}^{A})$	(8,4)(9,4)(7,6)
(346,1139)	(3.584,1.089)			(6,5)	$(eh_{33}^{D}, eh_{11}^{A})$	(9,2)
(346,1180)	(3.584,1.051)			(6,5)	$(eh_{33}^{D}, eh_{11}^{A})$	(8,6)
(346, ~1260)	(3.584,0.984)			(6,5)	$(eh_{33}^{D}, eh_{11}^{A})$	(9,5)(10,5)(8,7)
(337,1025)	(3.679,1.209)	(7,5)	(eh_{33}, eh_{11})			
(337,1060)	(3.679,1.170)			(7,5)	$(eh_{33}^{D}, eh_{11}^{A})$	(10,2)
(337, ~1116)	(3.679,1.111)			(7,5)	$(eh_{33}^{D}, eh_{11}^{A})$	(8,4)(9,4)(7,6)
(337,1139)	(3.679,1.089)			(7,5)	$(eh_{33}^{D}, eh_{11}^{A})$	(9,2)
(337,1180)	(3.679,1.051)			(7,5)	$(eh_{33}^{D}, eh_{11}^{A})$	(8,6)
(337, ~1260)	(3.679,0.984)			(7,5)	$(eh_{33}^{D}, eh_{11}^{A})$	(9,5)(10,5)(8,7)
(324,879)	(3.827,1.411)	(6,4)	(eh_{33}, eh_{11})			

λ_{ex} and λ_{em} are excitation and emission wavelengths in nm, E_{ex} and E_{em} are the excitation and emission energy in eV. (n, m) is the chirality. eh_{ii}^{D} ($i = 1, 2, 3, 4$) and eh_{11}^{A} are excitonic excitation of donors (D) and excitonic emission of acceptors (A), respectively.

this spectral range. On the other hand, we find that in Fig. 3(c), the PL peaks of (8,3), (6,5) and (7,5) tubes are mainly due to the PL emission associated to the resonant excitation of their eh_{11} sidebands. But, the PL peaks of (9,4), (8,4), (7,6) and (9,2) tubes near 1110 nm is determined by EET from (6,5) tubes, due to their higher concentration compared to (5,4), (6,4), (9,1) and (8,3) (see Fig. 3(a)).

After 2 months, the PL spectrum of the suspension decreases in intensity, broadens in spectral profile

Table 2
Assignment of the observed excitonic sidebands and corresponding EET-induced features in the one-photon PLE map of as-prepared CoMoCAT SWNT suspension in D_2O/SDBS

$(\lambda_{ex},\lambda_{em})$	(E_{ex},E_{em})	Phonon sidebands		EET features		
		(n,m)	Assign.	Donor	Assign.	Acceptor
(895,1060)	(1.385,1.170)	(10,2)	(eh_{11}^{ph}, eh_{11})			
(895, ~1116)	(1.385,1.111)			(10,2)	$(eh_{11}^{ph,D}, eh_{11}^{A})$	(8,4)(9,4)(7,6)
(871,1025)	(1.424,1.210)	(7,5)	(eh_{11}^{ph}, eh_{11})			
(871,1060)	(1.424,1.170)			(7,5)	$(eh_{11}^{ph,D}, eh_{11}^{A})$	(10,2)
(871, ~1116)	(1.424,1.111)			(7,5)	$(eh_{11}^{ph,D}, eh_{11}^{A})$	(8,4)(9,4)(7,6)
(837,980)	(1.481,1.265)	(6,5)	(eh_{11}^{ph}, eh_{11})			
(837,1025)	(1.481,1.210)			(6,5)	$(eh_{11}^{ph,D}, eh_{11}^{A})$	(7,5)
(837, ~1116)	(1.481,1.111)			(6,5)	$(eh_{11}^{ph,D}, eh_{11}^{A})$	(8,4),(9,4),(7,6)
(837,1139)	(1.481,1.088)			(6,5)	$(eh_{11}^{ph,D}, eh_{11}^{A})$	(9,2)
(837,1180)	(1.481,1.051)			(6,5)	$(eh_{11}^{ph,D}, eh_{11}^{A})$	(8,6)
(837, ~1260)	(1.481,0.984)			(6,5)	$(eh_{11}^{ph,D}, eh_{11}^{A})$	(9,5),(10,5),(8,7)
(788,914)	(1.574,1.357)	(9,1)	(eh_{11}^{ph}, eh_{11})			
(788,955)	(1.574,1.298)			(9,1)	$(eh_{11}^{ph,D}, eh_{11}^{A})$	(8,3)
(788,980)	(1.574,1.265)			(9,1)	$(eh_{11}^{ph,D}, eh_{11}^{A})$	(6,5)
(788,1025)	(1.574,1.210)			(9,1)	$(eh_{11}^{ph,D}, eh_{11}^{A})$	(7,5)
(788, ~1116)	(1.574,1.111)			(9,1)	$(eh_{11}^{ph,D}, eh_{11}^{A})$	(8,4),(9,4),(7,6)
(762,879)	(1.627,1.411)	(6,4)	(eh_{11}^{ph}, eh_{11})			
(762,914)	(1.627,1.357)			(6,4)	$(eh_{11}^{ph,D}, eh_{11}^{A})$	(9,1)
(762,955)	(1.627,1.298)			(6,4)	$(eh_{11}^{ph,D}, eh_{11}^{A})$	(8,3)
(762,980)	(1.627,1.265)			(6,4)	$(eh_{11}^{ph,D}, eh_{11}^{A})$	(6,5)
(762,1025)	(1.627,1.210)			(6,4)	$(eh_{11}^{ph,D}, eh_{11}^{A})$	(7,5)
(762,1060)	(1.627,1.170)			(6,4)	$(eh_{11}^{ph,D}, eh_{11}^{A})$	(10,2)
(762, ~1116)	(1.627,1.111)			(6,4)	$(eh_{11}^{ph,D}, eh_{11}^{A})$	(8,4),(9,4),(7,6)
(724,828)	(1.713,1.498)	(5,4)	(eh_{11}^{ph}, eh_{11})			
(724,879)	(1.713,1.411)			(5,4)	$(eh_{11}^{ph,D}, eh_{11}^{A})$	(6,4)
(724,955)	(1.713,1.298)			(5,4)	$(eh_{11}^{ph,D}, eh_{11}^{A})$	(8,3)
(724,980)	(1.713,1.265)			(5,4)	$(eh_{11}^{ph,D}, eh_{11}^{A})$	(6,5)
(724,1025)	(1.713,1.210)			(5,4)	$(eh_{11}^{ph,D}, eh_{11}^{A})$	(7,5)
(528,879)	(2.348,1.411)	(6,4)	(eh_{22}^{ph}, eh_{11})			
(528,914)	(2.348,1.357)			(6,4)	$(eh_{22}^{ph,D}, eh_{11}^{A})$	(9,1)
(528,1025)	(2.348,1.210)			(6,4)	$(eh_{22}^{ph,D}, eh_{11}^{A})$	(7,5)
(515,980)	(2.408,1.265)	(6,5)	(eh_{22}^{ph}, eh_{11})			
(515,1025)	(2.408,1.210)			(6,5)	$(eh_{22}^{ph,D}, eh_{11}^{A})$	(7,5)
(515, ~1116)	(2.408,1.111)			(6,5)	$(eh_{22}^{ph,D}, eh_{11}^{A})$	(8,4),(9,4),(7,6)
(515,1139)	(2.408,1.088)			(6,5)	$(eh_{22}^{ph,D}, eh_{11}^{A})$	(9,2)
(515,1180)	(2.408,1.051)			(6,5)	$(eh_{22}^{ph,D}, eh_{11}^{A})$	(8,6)
(515, ~1260)	(2.408,0.984)			(6,5)	$(eh_{22}^{ph,D}, eh_{11}^{A})$	(9,5),(10,5),(8,7)
(447,828)	(2.774,1.498)	(5,4)	(eh_{22}^{ph}, eh_{11})			
(447,980)	(2.774,1.265)			(5,4)	$(eh_{22}^{ph,D}, eh_{11}^{A})$	(6,5)
(447,1025)	(2.774,1.210)			(5,4)	$(eh_{22}^{ph,D}, eh_{11}^{A})$	(7,5)
(447, ~1116)	(2.774,1.111)			(5,4)	$(eh_{22}^{ph,D}, eh_{11}^{A})$	(8,4)(9,4)(7,6)

λ_{ex} and λ_{em} are excitation and emission wavelengths in nm, E_{ex} and E_{em} are excitation and emission energies in eV. (n, m) is the chirality. eh_{ii}^{ph} $(i = 1, 2)$ denotes the phonon sideband of eh_{ii}. $eh_{ii}^{ph,D}$ $(i = 1, 2)$ and eh_{11}^{A} are sideband excitation of donors (D) and excitonic emission of acceptors (A), respectively.

and red-shifts in emission wavelength, as shown in Figs. 3(b) and (c). This is consistent with the change of the absorption profiles of the suspensions with aging as shown in Fig. 3(a). Decrease in exciton–exciton resonance intensities suggests that small nanotube bundles in the pristine suspensions aggregate into bigger ones after 2 months. The EET-induced PL intensity of (9,4), (8,4), (7,6) and (9,2) acceptor tubes in Fig. 3(c) is found to be

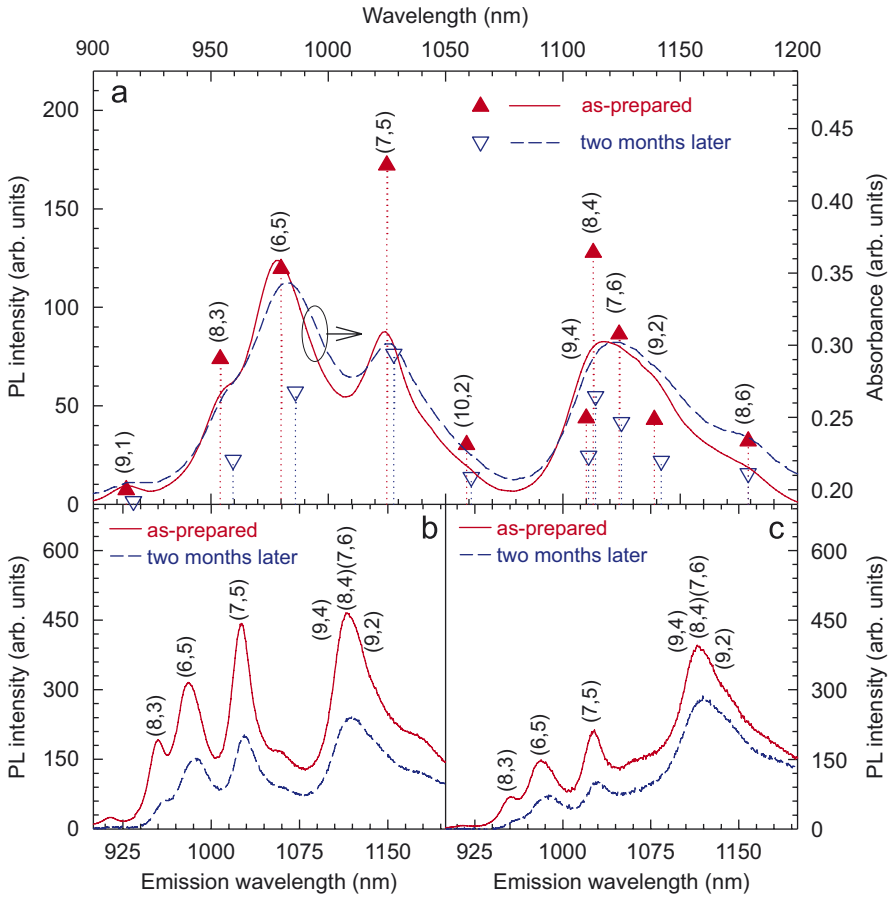

Fig. 3. (Color online). (a) Absorption spectra (solid and dashed lines) and PL intensity of each exciton–exciton resonance (▲ and ▽) of as-prepared suspension and after 2 months; (b) summed PL spectra with excitations between 420 and 780 nm of as-prepared suspension and after 2 months; (c) summed PL spectra with excitations between 780 and 999 nm of as-prepared suspension and after 2 months where all the (eh_{11}, eh_{11}) emissions are not included.

comparable with that of (8,3), (6,5) or (7,5) donor tubes from exciton–exciton resonances in Fig. 3(b), suggesting efficient energy transfer between nanotubes in bundles [7]. After 2 months of incubation, the EET-induced PL peaks at ~1115 nm in Fig. 3(c) are even stronger than those of exciton–exciton resonances in Fig. 3(b). This suggests that the efficiency of exciton energy transfer can remain very high even after the formation of bigger bundles. Therefore, the summed PL spectra over a wide excitation range can be a useful tool to study and characterize the formation of bundles.

4. Conclusions

In summary, we compared PL excitation and absorption spectra of the same nanotube suspensions over a period of 2 months. We showed that the nanotube suspensions aggregate into bigger bundles, as confirmed from the red-shift of PL and absorption spectra. The absorption profiles of as-prepared and incubated (2 months) suspensions are very similar. However, the PL excitation and the summed PL spectra over a wide excitation range are quite different even though the composition of both suspensions remain the same. This suggests that absorption measurement is a more reliable technique to reveal the concentration distribution of nanotube bundles compared to PL and PLE. This is because the formation of small bundles does not alter the absorption spectra, while it does change the PLE spectra. The new features detected in the PLE map of suspensions are associated with the nanotube bundles and assigned to energy transfer from excitons and excitonic phonon sidebands of donors to acceptors eh_{11}. These results can be used to characterize the existence and formation of nanotube bundles in suspensions.

Acknowledgments

The authors acknowledge funding from EPSRC Grants GR/S97613 and EP/E500935/1, and the Ministry of Information and Communication, Republic of Korea (Project no. A1100-0501-0073). P.H.T. and A.C.F. acknowledge funding from the Royal Society. A.C.F. acknowledges funding from the Leverhulme Trust. F.B. thanks P.G. Gucciardi for fruitful discussions.

References

[1] F. Wang, et al., Science 308 (2005) 838.
[2] J. Maultzsch, et al., Phys. Rev. B 72 (2005) 241402 (R).
[3] M.J. O'Connell, et al., Science 297 (2002) 593.
[4] S.M. Bachilo, et al., Science 298 (2002) 2361.
[5] A. Jorio, et al., Appl. Phys. Lett. 88 (2006) 023109.
[6] T. Okazaki, et al., Chem. Phys. Lett. 420 (2006) 286.
[7] P.H. Tan, et al., Phys. Rev. Lett. 99 (2007) 137402.
[8] S.M. Bachilo, et al., J. Amer. Chem. Soc. 125 (2003) 11186.
[9] V.C. Moore, et al., Nano Lett. 3 (2003) 1379.
[10] S. Reich, C. Thomsen, P. Ordejon, Phys. Rev. B 65 (2002) 155411.
[11] F. Wang, et al., Phys. Rev. Lett. 96 (2006) 167401.
[12] V. Perebeinos, J. Tersoff, P. Avouris, Phys. Rev. Lett. 94 (2005) 027402.
[13] F. Plentz, et al., Phys. Rev. Lett. 95 (2005) 247401.
[14] Y. Miyauchi, S. Maruyama, Phys. Rev. B 74 (2006) 035415.
[15] S. Reich, C. Thomsen, J. Robertson, Phys. Rev. Lett. 95 (2005) 077402.